Analysis of 3D filament structures in various magnetic configurations of the W7-X stellarator

A. Buzas[1,2], C. Biedermann[3], G. Cseh[1], B. Csillag[1], G. Kocsis[1], T. Szepesi[1], S. Zoletnik[1] and the W7-X Team *

[1] *Centre for Energy Research, Budapest, Hungary*

[2] *Institute of Nuclear Techniques, BME, Budapest, Hungary*

[3] *Max-Planck-Institute for Plasma Physics, Greifswald, Germany*

Filaments in fusion plasmas are high-density structures aligned with magnetic field lines and can be responsible for a significant portion of particle transport in the plasma edge. Their origin is often linked to density perturbations caused by interchange modes, in which curvature and ∇B drifts result in charge separation. This polarized structure is moved by the E $\times$ B drift [1]. Such filaments have been observed on W7-X by multiple diagnostics, including fast-cameras [2], alkali beam emission spectroscopy [3] and reciprocating probes [4]. Due to the complex magnetic geometry, a 3D treatment of these filaments is necessary. The W7-X fast-camera system [5] offers a tangential vantage point, from where both poloidal movement and toroidal structure are visible. The images analyzed here were recorded during OP1 in 2018, using a Photron fast camera, which via viewport AEQ21 can observe most of the poloidal cross-section of the plasma with up to 90 kHz sampling frequency (or higher, with a significant decrease in range of interest (ROI)). The light was filtered at the C III emission line, 465 nm (images filtered at the H_α line showed significantly less detail). The pixels were averaged over 3x3 grids (binned) to reduce noise and computational time, than filtered between 2 and 10 kHz. To highlight filament activity and geometry, pixel-wise correlations are calculated. This study mainly focuses on the time-delay of the maxima of these correlations. This makes it possible to pinpoint correlated areas and patterns of movement on a single picture. To put results in the context of the magnetic geometry, field lines and magnetic surfaces are plotted over the image. These are calculated by field line tracing from the equilibrium magnetic field and projected to image coordinates using linear transformations. On the example on Fig. 2 blue signify areas where the maximum of the cross-correlation relative to the reference point is at a negative time lag, while red means a positive time lag. White is where the maximum is at

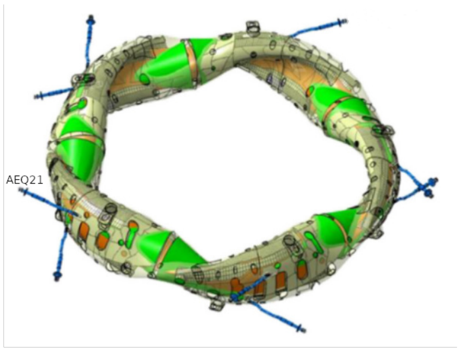

Figure 1: *W7X Fast Camera System*

*See Pedersen *et al* 2021 (https://doi.org/10.1088/1741-4326/ac2cf5) for the W7-X Team.

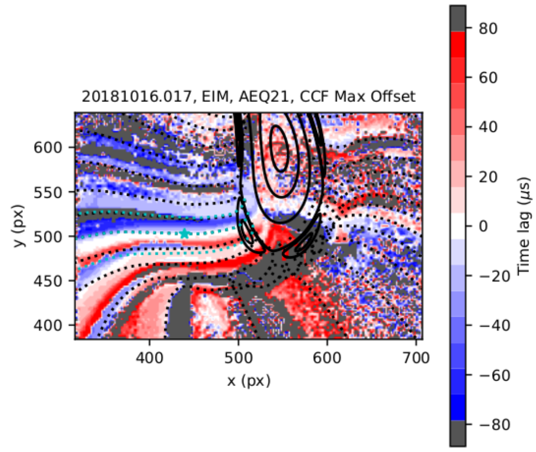

Figure 2: Time delay of correlation maxima

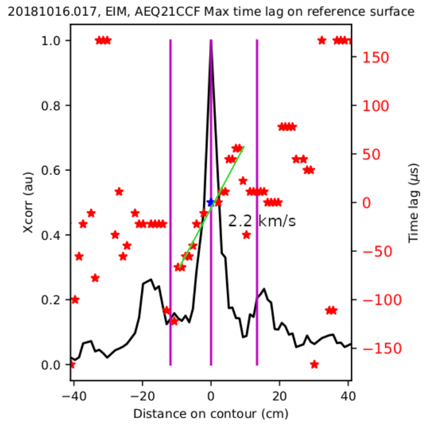

Figure 3: Max correlation and its time delay along a flux surface contour

zero time, while gray areas are so far removed, that they are unlikely to have any significance. Blue-white-red transition signifies movement. Turquoise shows the reference point (star) and the field line that it is on (dotted line). Fig. 3 shows the values of Fig. 2 along a flux surface contour at a certain toroidal coordinate (in red). The black line is the maximal correlation, the red stars are its time delay (1 and 0 at the reference point). The pink lines are the reference field line and it returning after one toroidal turnaround in both directions. The green line is a linear fit, that gives the poloidal velocity around the reference point (2.2 km/s in this instance).

There are various factors which makes the interpretation of the results difficult. Projected field lines intersect each other at various places, which makes distinguishing between structures and following their movement or measuring their speed quite challenging. Other perturbations interfere with filamental patterns as well, for example there are multiple toroidally rotating structures that follow field lines and cause similar patterns as filaments. Field lines that run parallel with the line of view appear more luminous and outshine other areas.

For this paper, results from the standard configuration (EIM-252) shot 20181016.015 are presented. It was recorded with 45 kHz framerate, the light was filtered to 465 nm. Both attached and detached plasma is observed. As Fig. 4 shows, filament activity happens at magnetic islands. Matching correlation patterns with field lines suggests, that they appear on the Last Closed Flux Surface (LCFS), not the islands themselves. Fig. 4, 6, 7 shows the appearance of patterns on returning field lines after a toroidal turn (with different reference points). It is supported by Fig. 5 as well, where increased correlation is present at the returning field line's position. Filaments in general move poloidally in a counter-clockwise direction at all locations around the plasma. This is not always the case however, as Fig. 6 shows, where the sequence of colours is reversed. Their velocities measured as demonstrated on Fig. 3 varied between 1 and 3 km/s, which agrees with expectations, though the accuracy of the method still needs improvement.

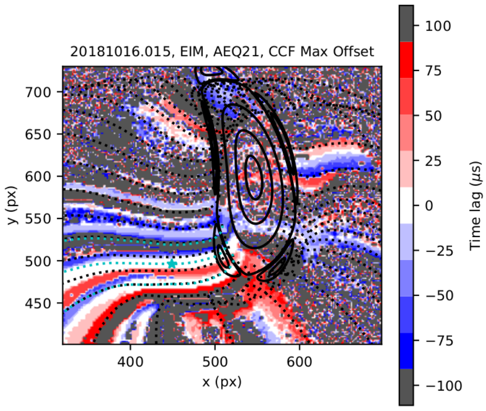

Figure 4: Patterns of filament activity

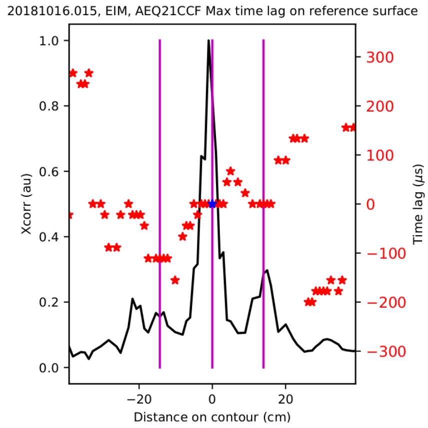

Figure 5: Values of Fig. 4 on a flux surface contour

In detachment there seem to be an increased filament activity. This results in more distinct patterns and higher correlation values, as shown on Fig. 4 and 7 (detachment) and Fig. 6 (attachment). Greater activity will also result in patterns appearing at not necessarily strongly correlated, but otherwise similarly active areas. Patterns in detachment seem to be more aligned with the field lines of surfaces inside (but still close to) the LCFS. This claim is also supported by the observation of reversed movement mentioned earlier. The same thing was seen at the same location in the shots 20181016.016 and 20181016.017 as well. E_r changes sign at the separatrix [6], which means E×B driven flows will change direction too. This indicates, that filaments that are observed by the fast camera switch sides at the LCFS at that location in detachment. In the absolute values of velocity, there's no sign of significant change around the plasma.

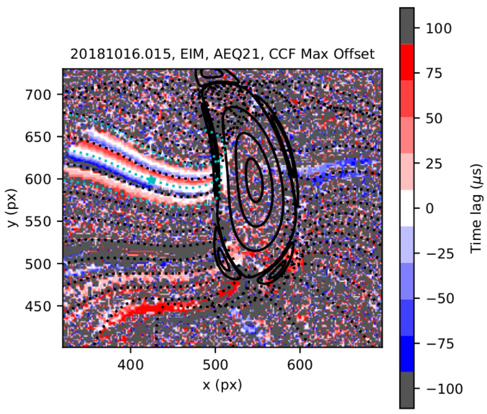

Figure 6: Time delay patterns in attachment

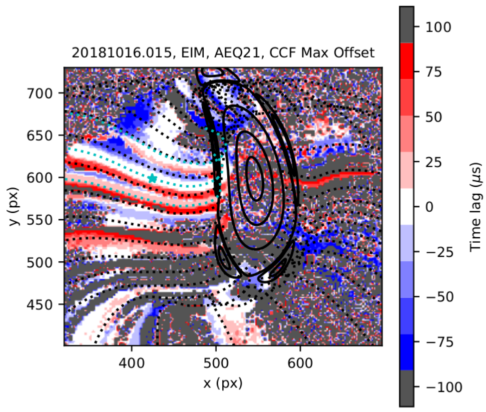

Figure 7: Time delay patterns in detachment at the same reference point as Fig. 6

For high ι configuration (FTM-252) no real good quality shot was found so far. The one presented here is 20180822.023. It was recorded with 45 kHz framerate. Filament activity seems to occur around the islands here as well, however due to the low quality, patterns are less clear and determining velocity is nigh impossible. The few instances, where a line could be fitted, yielded

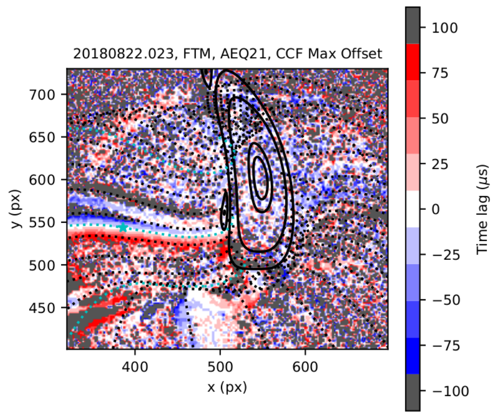

Figure 8: Patterns of filament activity at island 1

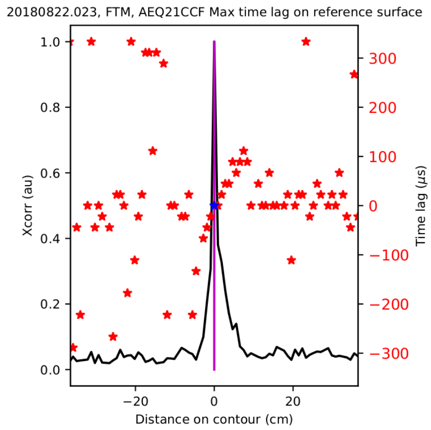

Figure 9: Values of Fig. 8 on a flux surface contour

similar or slower values than in standard configuration, but there were not enough of these to be conclusive. The most important difference however is that there is no sign of any significant correlation on returning field lines.

In this study, the capabilities of fast cameras were successfully demonstrated for the observation of filaments. Filaments appear at magnetic islands, around the LCFS in both standard and high ι configurations. They aligned with field lines well, even for a toroidal turnaround (at least in standard configuration). There seems to be an increased activity in detachment. Plotting the time-delay of the max correlation between pixels reveals patterns of movement and helps measuring poloidal velocity, which was found to fall in the 1-3 km/s range, which (assuming it is E×B driven) at 2.5 T corresponds to roughly ∼5000 V/m E_r. This technique however still needs refinement. Moving forward, more discharges should be examined with varying parameters, especially in high and low ι configurations. The signals of other diagnostics (such as A-BES and reflectometry) could be compared to the parts of the images, which they are connected to by field lines, to further explore 3D behaviour. *

References

[1] D'Ippolito D. A. *et al* Phys. Plasmas **18**, 060501 (2011)

[2] Kocsis G. *et al* 44th EPS Conf. on Plasma Phys. ECA vol. **41F**, O2.102 (2017)

[3] Zoletnik S. *et al* Plasma Phys. Control. Fusion **62**, 014017 (2020)

[4] Killer C. *et al* Plasma Phys. Control. Fusion **62**, 085003 (2020)

[5] Kocsis G. *et al* Fus. Eng. Des. **96-97**, 808, (2015)

[6] Carralero D. *et al* Nucl. Fusion **60**, 106019, (2020)

*This work has been carried out within the framework of the EUROfusion Consortium, funded by the European Union via the Euratom Research and Training Programme (Grant Agreement No 101052200 — EUROfusion). Views and opinions expressed are however those of the author(s) only and do not necessarily reflect those of the European Union or the European Commission. Neither the European Union nor the European Commission can be held responsible for them.